Article

Genetic Algorithm for Optimal Placement of Steel Plate Shear Walls for Steel Frames

Jianian He [1], Shuhong Lin [1], Yicheng Li [1], Xian Dong [2] and Shizhe Chen [1],*

[1] School of Civil and Transportation Engineering, Guangdong University of Technology, Guangzhou 510006, China; jnhe@gdut.edu.cn (J.H.); linshuhongsteel@163.com (S.L.); 2112009128@mail2.gdut.edu.cn (Y.L.)

[2] School of Civil Engineering, Shi Jiazhuang Tiedao University, Shi Jiazhuang 050043, China; wendongxian@163.com

* Correspondence: chensz@gdut.edu.cn

Abstract: Frame structures equipped with steel plate shear walls (SPSWs) have been widely used in high-rise buildings due to their good seismic performance. In this study, the strip model and combined strip model were used to analyze the performance of SPSWs. Furthermore, an improved genetic algorithm (IGA) was established to optimize the steel frame for 5, 10, and 20 stories. For each layer, layout optimization was conducted to determine the best configurations of the SPSWs, and two cases of size optimizations of conventional SPSW configurations in the frame were conducted. Results indicate the following: (i) the total weight of the five-story steel frame of layout optimization to determine the best SPSW configuration was approximately 10% lighter than those of the size optimization of conventional SPSW configurations, and this proportion gap expanded to approximately 15–25% for the 10-story and 20-story steel frames; (ii) the steel frame weight could be significantly reduced if the average percentages of story shear resisted by web plates are increased; and (iii) in the steel frame of layout optimization, the structural elements, especially the plate elements, were better utilized than those of size optimization when their inter-story drift ratios met the specification requirements. These results highlight the prominent performances of some important indicators of the design of an SPSW system with the layout optimized using IGA.

Keywords: steel frame; steel plate shear walls; optimal design; improved genetic algorithm; layout optimization

1. Introduction

Structural engineering design must meet safety, reliability, and economic savings. Therefore, the suitable optimization of engineering structures is needed to obtain the optimal balance between safety and economy. However, obtaining an effective algorithm is considered to be a major challenge in the optimization process owing to factors such as the large number of variables and implicit functions, highlighted nonlinearity, and the statical indetermination of the structures. Considerable research to design pure steel frames or steel bracing frames using meta-heuristic optimization algorithms has been conducted [1–10].

The optimization of a steel frame must consider both size and layout. Togan [1] reported on a design method employing teaching–learning-based optimization for the discrete size optimization of planar steel frames, which was demonstrated to be superior to other meta-heuristic algorithms. Çarbaş [2] proposed a biogeography-based optimization (BBO) for the discrete optimum design of real-size steel space frames. The steel frame structure optimized by BBO was lighter than those optimized by other algorithms and the robustness of BBO was also proved. Similarly, Kaveh and Farhoudi [3] used an approximate optimum steel design (AOSD) method for the layout optimization of braces for planar steel frames. The efficiency and accuracy of AOSD have been numerically demonstrated. Furthermore, Kaveh and Farhoudi [4] used several meta-heuristic algorithms for

the layout optimization of steel-braced frames. The results of their study revealed the similarity of these algorithms and that the convergence rate can be adjusted by generating some random answers to avoid sticking at locally optimal solutions. Liang et al. [5] presented a performance-based optimization method to develop an optimal topology design of bracing systems, where two demonstrations were used to show the efficiency of the method. Bagherinejad and Haghollahi [6] used topology optimization to determine the best configuration for a perforated steel plate shear wall (SPSW), where the thicknesses and length-to-height ratios of three plates were considered. Gholizadeh and Fattahi [7] proposed a modified particle swarm optimization algorithm to optimize tall steel buildings. Two cases were implemented to investigate the efficiency of their method. Farzampour et al. [8] used the grey wolf algorithm in the shape optimization of the butterfly-shaped shear links in the steel frame. The dissipation energy capability of the butterfly-shaped links was maximized, and the concentration of plastic strains was effectively reduced.

Current research on the layout and size optimization of multi-story and high-rise structures has proved the advantages of various new algorithms in many aspects. A one-dimensional element is also mature. However, these studies did not use two- or three-dimensional elements. Moreover, there are few cases involving the use of component-simplified models.

SPSW structures have been widely adopted in high-rise buildings owing to their good ductility, energy dissipation, and seismic performance [11]. Therefore, research on the optimization of steel frames with SPSWs is expected to increase in the future. An SPSW comprises an infilled steel plate connected to the surrounding beams and columns called the horizontal and vertical boundary elements, respectively. Currently, the studies on SPSWs are focused on the performance of different types of SPSWs [12–15], the effect of the surrounding frame on the performance of an SPSW system [16–20], and a simplified analysis model of an SPSW [21–24]. However, only a few studies have examined the optimal design of steel frames with SPSWs. Gholizadeh and Shahrezaei [25] used a bat algorithm for the layout optimization of a steel frame with SPSWs, and six cases were demonstrated to illustrate its effectiveness. However, they did not consider the structural constraints of the beam–column members or extend the method to high-rise structures.

In a design of a usual engineering program, the SPSW form was determined using traditional design method, and the section sizes of the components were then optimized. However, this process ignored the cooperative interaction between the frame and the SPSW, which caused the design to not be an authentic optimization in addition to lacking an accurate economic guide. Therefore, starting from the structural system, this study not only considered the geometric position of the shear wall, but also optimized the size of the components to explore and determine better structural forms.

In this study, the optimal design of steel frames with SPSWs was considered through an improved genetic algorithm (IGA) using a direction-based heuristic crossover operator (DBHX), substitution operation, adaptive mutation operator, and an elite scheme. The strip model (SM) and combined strip model (CSM) proposed in AISC 341-2010 [26] and JGJ/T 380-2015 [27], respectively, were used to model the SPSW performance. Three optimization cases of 5-, 10-, and 20-story steel frames were implemented to investigate the performance of steel frames with conventional and optimal SPSW configurations. For each layer, two cases of size optimization of the steel frame with conventional SPSW configurations and one case of layout optimization were conducted to determine the optimal position of the SPSW in the steel frame.

2. Introduction of Methods

2.1. Simplified Analysis Model of SPSWs

Recently, unstiffened SPSWs have been commonly applied to high-rise buildings. These types of SPSWs buckle when the lateral loads are light. The post-buckling performance of unstiffened SPSWs has been investigated in many aspects [28]. Although a shell element can be used to model the SPSW behavior, it is difficult to use a shell element when

designing a building. Issues arise such as convergence difficulty and time-consuming calculations so that many design software systems lack the capability to analyze the plastic and post-buckling performance of shell members. Therefore, many simplified analytical models for SPSWs have been developed in recent years. The SM and orthotropic membrane model (OMM) are recommended in AISC 341-2010 [26] and CAN/CSA S16.1-01 [29], respectively. The CSM is recommended in JGJ/T 380-2015 [27]. Studies [30] show that the SM and OMM can accurately model the performance of an SPSW when the height-to-thickness ratio (λ) is large; however, the result is relatively conservative when λ is less than 300. Furthermore, CSM3-7 and CSM2-8 (CSM models where 3 and 2 are the numbers of tension–compression strips, and 7 and 8 are the numbers of tension-only strips) can model the performance of SPSWs when λ varies from 100 to 300 and from 300 to 600, respectively. Therefore, this study used the SM and CSM to model the performance of SPSWs for different values of λ. The angles of the strips (α) in the SM and CSM are generally 39–45° if the column moment stiffnesses are above the minimum stiffness requirement. Several studies have shown that α is not significantly sensitive to the SPSW performance [21–23,30]. Therefore, for the convenience of modeling, α was assumed to be 45° in this study.

Table 1 and Figure 1 show the parameters and schematic of the simplified analysis model, respectively. The SM and CSM are switched by adjusting the number of tension–compression strips. The cross-sectional area of the strips can be calculated as [24,27]:

$$A = \frac{t_w \sqrt{L_e^2 + H_e^2}}{n} cos\left[45° - tan^{-1}\left(\frac{H_e}{L_e}\right)\right] \tag{1}$$

where t_w is the thickness of the web plates; H_e and L_e are the clear height and length of the web plates, respectively; and n is the number of one-way strips.

Table 1. Parameters of simplified analysis model of steel plate shear wall (SPSW).

λ	Simplified Analysis Model	m^*	l	α
$100 \leq \lambda \leq 300$	CSM3-7	7	3	45°
$300 \leq \lambda \leq 600$	CSM2-8	8	2	45°
$\lambda > 600$	SM	10	0	45°

m^*: number of tension-only strips; l: number of tension–compression strips.
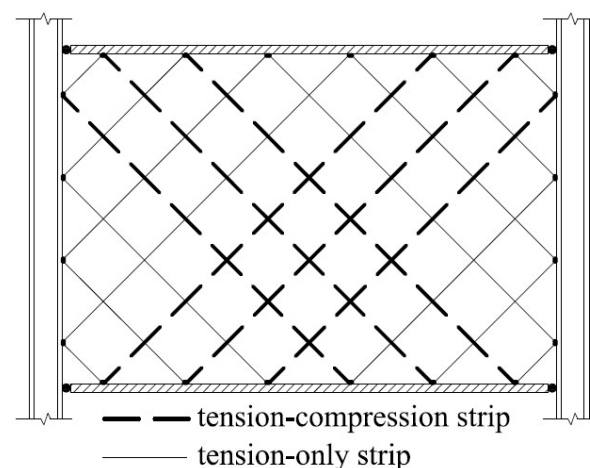
Figure 1. Simplified analysis model of SPSW.

2.2. Formulation of the Optimization Problem

In the optimal design of a steel frame with SPSWs, the summarized objective of the mathematical model is to minimize the overall weight of the structure, ensuring that all constraints in this study are satisfied. The mathematical model can be expressed as: Minimize:

$$W = \sum_{i=1}^{ngf} \rho A_i \sum_{m=1}^{nf} l_m + \sum_{j=1}^{ngp} \rho t_{wj} T_j \sum_{t=1}^{np} L_t h_t \tag{2}$$

where *ngf* and *ngp* are the number of frame elements and SPSW groups, respectively; *nf* and *np* are the number of frame elements in the i_{th} frame element and j_{th} SPSW group, respectively; ρ is the density of steel; A_i is the cross-sectional area of the i_{th} frame element group section; l_m is the length of the m_{th} frame element in the i_{th} group; t_{wj} is the thickness of the j_{th} SPSW group; T_j is the topological position variable of the j_{th} SPSW group; L_t is the length of the t_{th} SPSW in the j_{th} group; and h_t is the height of t_{th} SPSW in the j_{th} group.

The main constraints of the model can be expressed as follows:

- Strength and stiffness constraints of the frame element [31]

$$\sigma_i \leq \frac{f}{\gamma_{RE}}, \quad i = 1, 2, \ldots, ngf \tag{3}$$

$$\lambda_i \leq \lambda_{iu}, \quad i = 1, 2, \ldots, ngf \tag{4}$$

where σ_i is the strength of the *i*th element, *f* is the strength design value of steel, γ_{RE} is the seismic adjustment coefficient of the bearing capacity of the element, λ_i is the mid-span deflection value of the beam or maximum slenderness ratio of the column of the *i*th element, and λ_{iu} is the limit of λ_i.

- Inter-story drift ratio constraint [32]

$$\frac{(\delta_i - \delta_{i-1})}{h_i} \leq \delta_{iu}, \quad i = 1, 2, \ldots, n \tag{5}$$

where δ_i is the displacement of the *i*th frame, h_i is the height of the *i*th layer, δ_{iu} is the limit of interlayer displacement, and *n* is the total number of layers in the steel frame. Here, $\delta_{iu} = 0.004$.

- Shear bearing capacity constraint of SPSWs [27]

$$V \leq V_u \tag{6}$$

$$V_u = 0.42 f t_w L_e \tag{7}$$

where *V* is the shear design value of SPSWs, V_u is the design value of the shear capacity of SPSWs, *f* is the design value of the tensile, compressive, and flexural strengths of steel, t_w is the thickness of the web plates, and L_e is the clear length of the plates.

- Inertia moment constraint of the edge column and edge beam of SPSWs [27]

$$I_c \geq (1 - \kappa) \cdot I_{cmin} \tag{8}$$

$$I_{cmin} = \frac{0.0031 t_w H_c^4}{L_b} \tag{9}$$

$$I_b \geq I_{bmin} \tag{10}$$

$$I_{bmin} = \frac{0.0031 t_w L_b^4}{H_c} \tag{11}$$

where I_c and I_b are the moment of inertia of the edge column and edge beam, respectively; κ is the shear force distribution coefficient; I_{cmin} and I_{bmin} are the minimum moment of inertia of the edge column and edge beam, respectively; H_c is the height of the column; and L_b is the beam length.

- Construction constraints
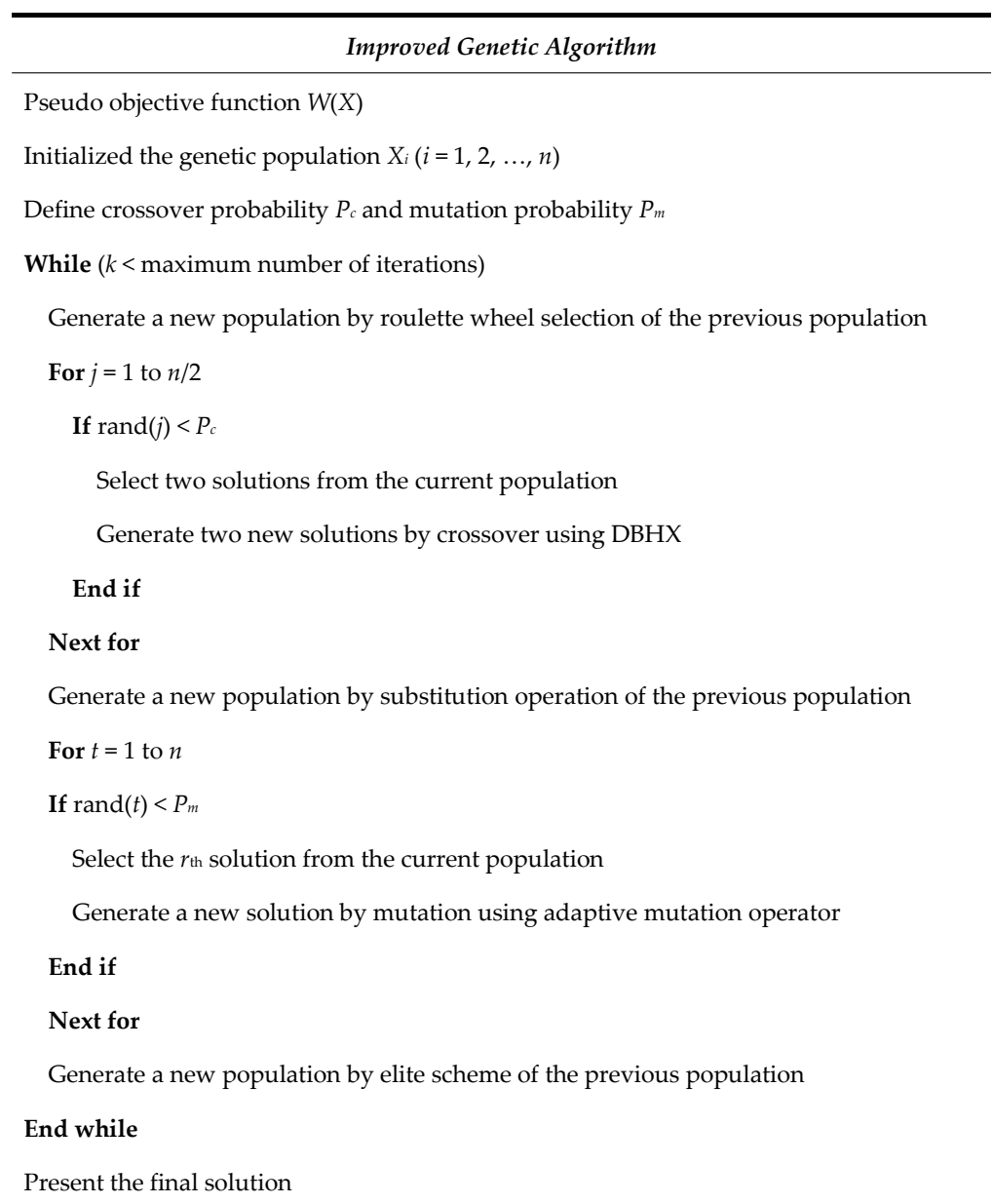
$$B_{bn} \leq B_{cn}, \quad n = 1, 2, \ldots, p \tag{12}$$

$$B_{ut} \leq B_{lt}, \quad t = 1, 2, \ldots, p - pb \tag{13}$$

$$H_{ut} \leq H_{lt}, \quad t = 1, 2, \ldots, p - pb \qquad (14)$$

where B_{bn} and B_{cn} are the beam and column flange widths at the nth node, respectively; B_{ut} and B_{lt} are the flange widths of the upper and lower columns, respectively; H_{ut} and H_{lt} are the section heights of the upper and lower columns, respectively; and p and pb are the total numbers of nodes in the structures and top structures, respectively.

2.3. IGA

Although several studies have demonstrated the robustness and applicability of the simple genetic algorithm (SGA), it certainly has some disadvantages, such as its slow search speed and tendency to fall into local optima. To overcome these issues, an IGA was established by introducing a DBHX [33], substitution operation [33,34], adaptive mutation operator [35], and elite scheme [36]. Figure 2 shows the pseudocode of the IGA used in this study.

Improved Genetic Algorithm

Pseudo objective function $W(X)$

Initialized the genetic population X_i (i = 1, 2, …, n)

Define crossover probability P_c and mutation probability P_m

While (k < maximum number of iterations)

  Generate a new population by roulette wheel selection of the previous population

  For j = 1 to $n/2$

    If rand(j) < P_c

      Select two solutions from the current population

      Generate two new solutions by crossover using DBHX

    End if

  Next for

  Generate a new population by substitution operation of the previous population

  For t = 1 to n

  If rand(t) < P_m

    Select the rth solution from the current population

    Generate a new solution by mutation using adaptive mutation operator

  End if

  Next for

  Generate a new population by elite scheme of the previous population

End while

Present the final solution

Figure 2. Pseudocode of the improved genetic algorithm (IGA).

2.3.1. DBHX

Usually, offspring individuals are easily trapped in parent individuals. To solve the problem, the DBHX method was proposed. A DBHX [33,34] can use the fitness value and crossover direction to obtain a better offspring. This operator not only overcomes the trap of local optimal solutions but also expands the search scope to avoid falling into the local optimal solution.

We denote the father individuals by X^a and X^b, in which X^b is more optimal than X^a. They produce two offspring individuals, respectively, Y^a and Y^b, where:

$$Y_i^a = X_i^a + \lambda \times r_i^a \times \vec{D} \tag{15}$$

$$Y_i^b = X_i^b + \lambda \times r_i^b \times \vec{D} \tag{16}$$

$$\vec{D} = X_i^b - X_i^a \tag{17}$$

$$r_i^a \in [0, 1] \tag{18}$$

$$r_i^b \in [0, 1] \tag{19}$$

$$i = 1, 2, \ldots, n \tag{20}$$

where $r_i^a \times \vec{D}$ and $r_i^b \times \vec{D}$ is the crossover directions, λ is the step size, $\lambda = 1$, and n is the total number of the variables of an individual.

Assuming the optimal solution of a design variable is X^*, the best crossover direction of X^a is $\vec{Y}$ ($X^* = X^a + \vec{Y}$), and the best crossover direction of X^b is $\vec{Z}$ ($X^* = X^b + \vec{Z}$). The DBHX can generate a crossover direction that is close to $\vec{Y}$ and $\vec{Z}$ although it is not the same as $\vec{Y}$ or $\vec{Z}$. Then, a better offspring individual would be generated with greater probability and the convergence speed of the algorithm would be improved.

2.3.2. Substitution Operation

As the number of iterations increases, an increasing number of the same or similar individuals appear, which reduces the diversity of the population and affects the search ability of the algorithm in the later stages. As a result, the algorithm cannot converge to the global optimal solution. To avoid this situation, a substitution operation was introduced here to ensure population diversity. This operation is described as follows: if there are two or more identical individuals in the crossover population, only one of the same individuals is retained, while the others are regenerated as new individuals.

2.3.3. Adaptive Mutation Operator

Assuming the parent individual is $y = [y_1, y_2, \ldots, y_n]$ and the offspring individual is $x = [x_1, x_2, \ldots, x_n]$, where [35]:

$$x_i = y_i - m_t(y_i - Min) + rm_t(Max - Min) \tag{21}$$

$$m_t = 1 - r^{[1 - \frac{t}{T}]^b} \tag{22}$$

$$x_i \in [y_i - m_t(y_i - Min), \ y_i + m_t(Max - y_i)] \tag{23}$$

Here, m_t is the coefficient of mutation, T is the maximum number of iterations of the algorithm, t is the current iteration number, b is a relevant parameter, $r \in [0,1]$, and *Min* and *Max* are the minimum and maximum values of the interval of the element y_i, respectively.

When the number of iterations is small, m_t is extremely close to 1 and the mutation operator has a large search range. As the number of iterations increases, m_t gradually decreases. The search range of the mutation operator becomes narrow, which improves the search speed in the later stages of the algorithm and saves the calculation overhead.

2.3.4. Elite Scheme

The elite scheme of this study is divided into two parts: (i) selecting N optimal individuals in the upper generation population and TN-N optimal individuals through genetic manipulation as the evolutionary populations of the next generation to retain the optimal individuals of each generation, where TN is the total number of individuals in the population; and (ii) comparing the optimal individual of each generation with the best individual of the previous generation. If the contemporary optimal individual is better, the optimal individual of the previous generation must be replaced with the contemporary one. Otherwise, the optimal individual of the previous generation would remain unchanged.

3. Numerical Examples

In this study, nine cases of three-bay steel frames with different layers were optimized using the IGA, which included six cases of size optimization of the usual fixed configurations of SPSWs in steel frames and three cases of layout optimization to determine the optimum placement of SPSWs in steel frames. The optimizations were implemented using the MATLAB and Ansys software packages [37,38]. Figure 3 shows a flow chart of the optimization of the steel frame with SPSWs. The values of the modulus of elasticity, Poisson's ratio, and weight density used in this study were $E = 206$ GPa, $\nu = 0.3$, and $\rho = 7850$ kg/m^3, respectively. An Ansys element, BEAM189, was used to model the performance of the beam and column, and an Ansys element, LINK180, was used to model the performance of the tension-only and tension–compression strips of the simplified analysis model of SPSWs. The column foots were all fixed as the boundary of each frame. Additionally, all the beam–column joints were also fixed.
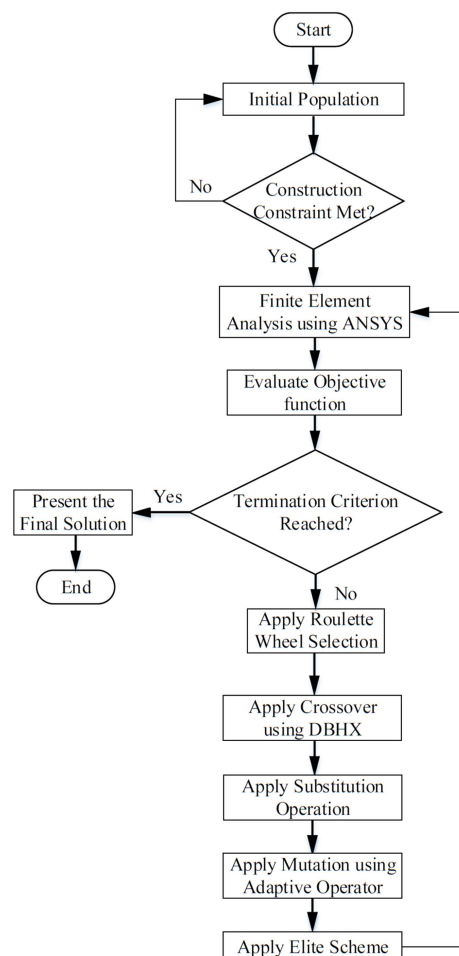
Figure 3. Flow chart of optimization of steel frame with SPSWs by IGA.

The sections of the beam and column elements were assumed to be selected from the welded steel H-section in YB 3301 (2005) [39]. The lower and upper bounds on the SPSW thickness of the 5- and 10-story steel frames were 1.0 and 10.0 mm, respectively; on the contrary, the lower and upper bounds of the 20-story steel frame were 1.0 and 15.0 mm, respectively. Both the SM and CSM were used to model the performance of the SPSWs with different height-to-thickness ratios. Table 2 summarizes the parameters of the model.

Table 2. Simplified analysis model of SPSW with different λ.

Thickness of SPSWs (mm)	λ	Simplified Analysis Model
$1.0 \leq t_w \leq 6.6$	$\lambda > 600$	SM
$6.7 \leq t_w \leq 10.0$	$400 \leq \lambda \leq 600$	CSM2-8
$13.4 \leq t_w \leq 15.0$	$266 \leq \lambda \leq 300$	CSM3-7

The calculating method of the earthquake loading for all frames was as follows:

- A uniformly distributed gravity load of 30 kN/m was applied to all the beam elements;
- The earthquake loads were calculated according to GB 50011-2010 [32]. Assuming that the building is located in an 8-degree seismic fortification zone, the basic acceleration of the design earthquake was 0.2 g. The type of construction site soil was determined as type II. The design earthquake classification was the first group. Equivalent base shear method was used to calculate the values of the earthquake loads acting on each story of each frame. The gravity P–Δ effect was considered during the calculation.

Table 3 summarizes the values of the earthquake loads acting on structures with different layers.

Table 3. Earthquake load acting on 5-, 10-, and 20-story steel frames.

| Floor	Earthquake Loads (kN)		
	5-Story Steel Frame	10-Story Steel Frame	20-Story Steel Frame
1	87.77	33.66	9.73
2	175.54	67.32	19.46
3	263.3	100.98	29.19
4	351.07	134.64	38.92
5	438.84	168.31	48.65
6	-	201.97	58.38
7	-	235.63	68.11
8	-	269.29	77.84
9	-	302.95	87.57
10	-	336.61	97.3
11	-	-	107.03
12	-	-	116.76
13	-	-	126.49
14	-	-	136.22
15	-	-	145.95
16	-	-	155.68
17	-	-	165.41
18	-	-	175.15
19	-	-	184.88
20	-	-	194.61
Base shear	1316.52	1851.36	2043.33

To accelerate optimization, a birth–death element was introduced to simulate the arrangement and removal of SPSWs in the layout optimization of the steel frames. In the new iteration, all LINK180 elements are activated, followed by deleting the elements using a birth–death element depending on the optimized layout of SPSWs of every individual in the population.

3.1. Nine Structure Models with Different Layers

Figures 4–6 illustrate the 5-, 10-, and 20-story steel frames used in this study, their element grouping details, and two usual fixed configurations of the SPSWs in the frame, respectively. The genetic parameters of the model are listed in Table 4. The three following optimization cases were considered for each steel frame:

- Size optimization of the steel frame with a fixed configuration of the SPSW with different layers, denoted as SPSW1-5, SPSW1-10, and SPSW1-20 for 5-, 10-, and 20-story steel frames, respectively.
- Size optimization of the steel frame with a fixed configuration of the SPSW with different layers, denoted as SPSW2-5, SPSW2-10, and SPSW2-20 for 5-, 10-, and 20-story steel frames, respectively.
- Layout optimization of the steel frame to determine the optimal configuration of the SPSW with different layers, denoted as SPSW3-5, SPSW3-10, and SPSW3-20 for 5-, 10-, and 20-story steel frames, respectively. To validate the effectiveness of the IGA, a case of layout optimization of the five-story steel frame, SPSW3-5-SGA, was conducted to determine the optimal configuration of the SPSW using SGA.
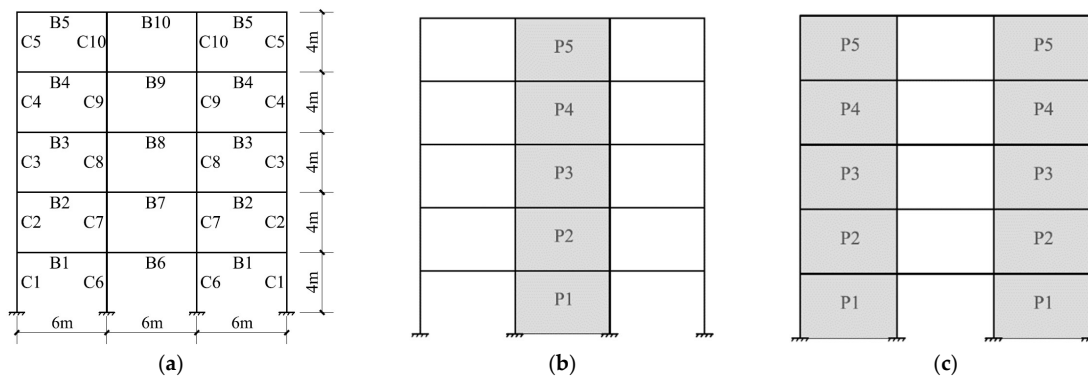
Figure 4. Five-story steel frame: (**a**) element group numbers; (**b**) SPSW1-5; and (**c**) SPSW2-5.
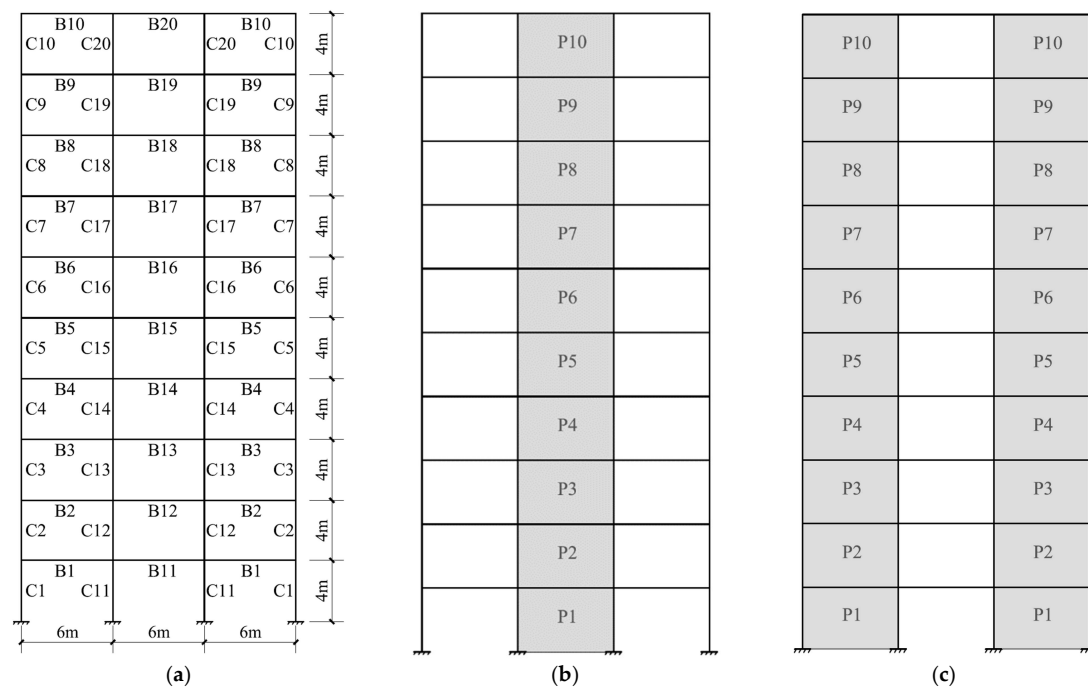
Figure 5. Ten-story steel frame: (**a**) element group numbers; (**b**) SPSW1-10; and (**c**) SPSW2-10.
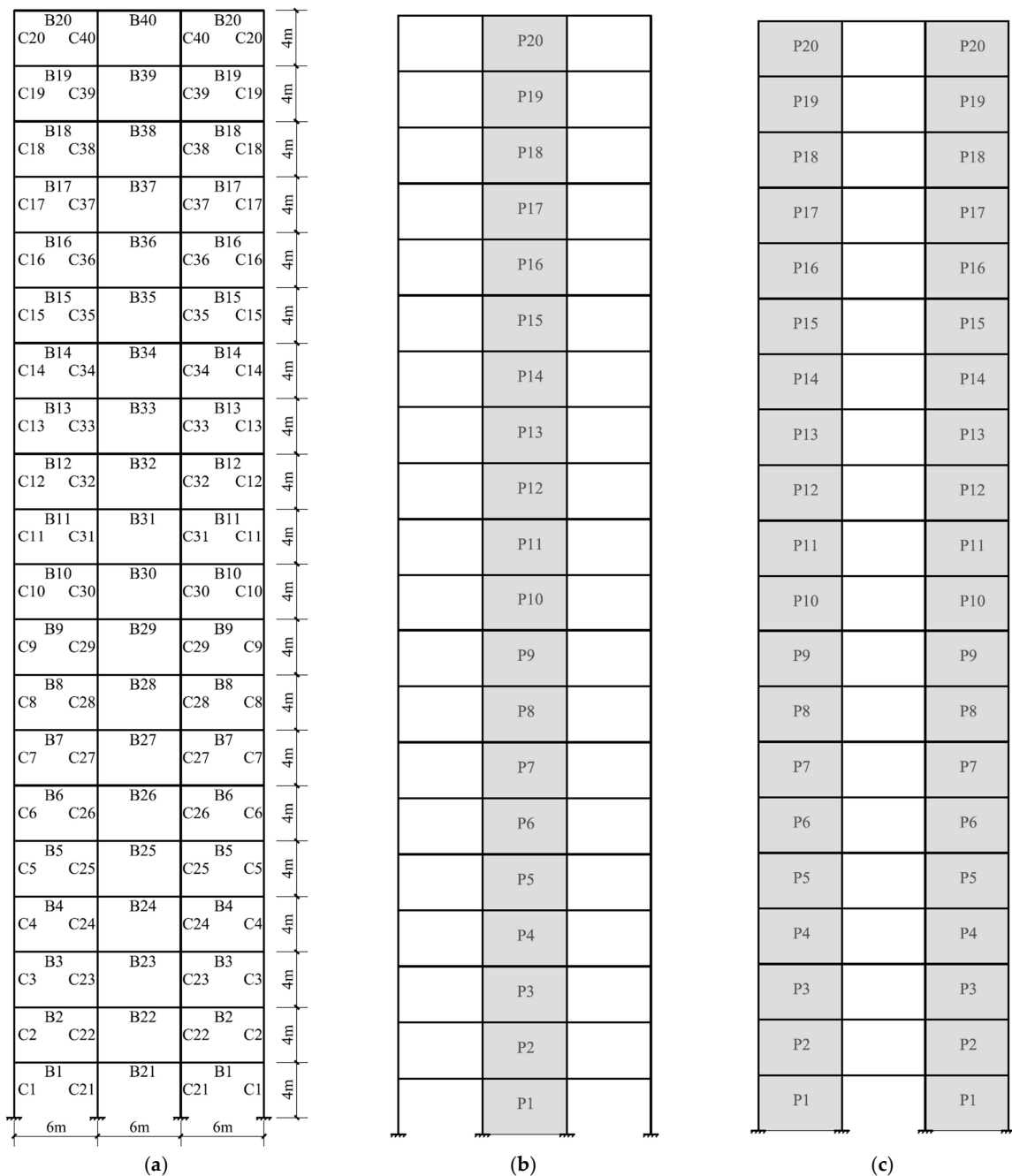
Figure 6. Twenty-story steel frame: (**a**) element group numbers; (**b**) SPSW1-20; and (**c**) SPSW2-20.

Table 4. Genetic parameters of structures with different stories.

Steel Frame	Number in Population	Genetic Iterations	Cross Probability	Mutation Probability
5-story	200	150	0.8	0.4
10-story	200	200	0.8	0.4
20-story	200	300	0.8	0.5

3.2. Optimization Results of Five-Story Steel Frame

The best configuration of the SPSW determined through layout optimization using the IGA and SGA is shown in Figures 7 and 8, respectively. The convergence histories of the five-story steel frame for SPSW1-5, SPSW2-5, SPSW3-5, and SPSW3-5-SGA are shown in Figure 9. Table 5 summarizes the optimum results obtained for each case.
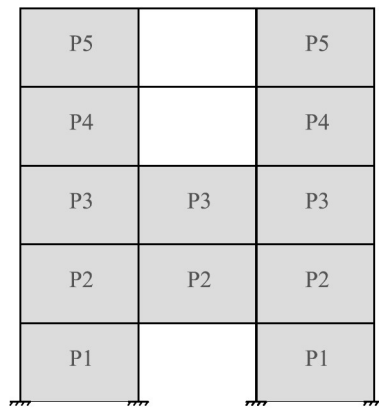
Figure 7. Best configuration of SPSW3-5.
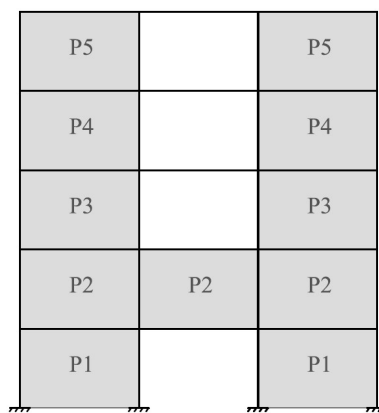
Figure 8. Best configuration of SPSW3-5-SGA.
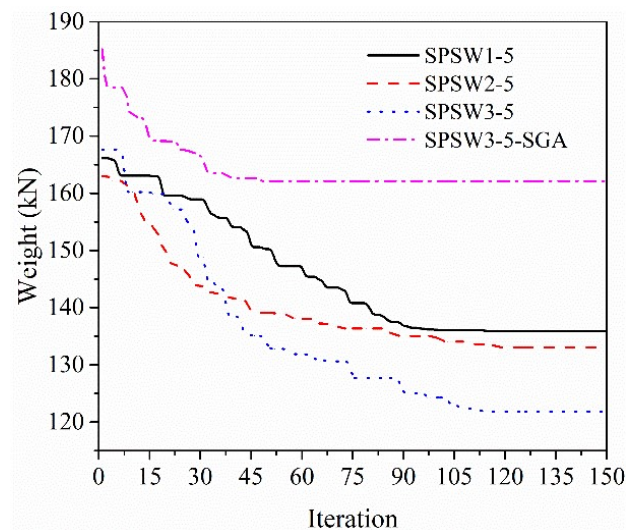
Figure 9. Convergence histories of 5-story steel frame.

Table 5 and Figure 9 indicate that the optimum weights of SPSW3-5 were 10.4% and 8.45% lighter than those of SPSW1-5 and SPSW2-5, respectively. The percentages of the story shear resisted by the steel plate are listed in Table 6. The average for SPSW3-5 (59.25%) was higher than that for SPSW1-5 (58.01%) and SPSW2-5 (59.18%); this indicates that the frame weight can be significantly reduced when the average percentage of story shear resisted by the steel plate increases.

Table 5. Optimum designs of SPSW1-5, SPSW2-5, SPSW3-5, and SPSW3-5-SGA.

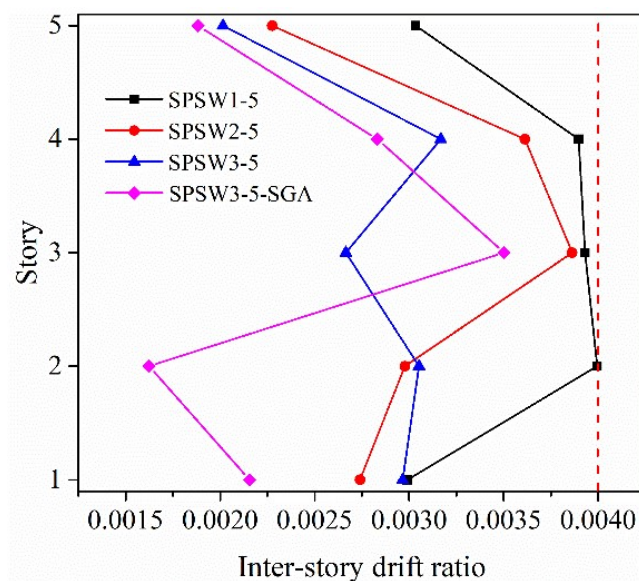| No.	Optimum Designs				No.	Optimum Designs			
	SPSW1-5	SPSW2-5	SPSW3-5	SPSW3-5-SGA		SPSW1-5	SPSW2-5	SPSW3-5	SPSW3-5-SGA
C1	WH 400 × 200	WH 600 × 400	WH 500 × 300	WH 500 × 300	B5	WH 300 × 200	WH 600 × 300	WH 600 × 300	WH 600 × 300
C2	WH 350 × 200	WH 350 × 350	WH 300 × 300	WH 400 × 300	B6	WH 400 × 200	WH 300 × 200	WH 600 × 300	WH 800 × 300
C3	WH 300 × 200	WH 350 × 300	WH 300 × 300	WH 350 × 300	B7	WH 400 × 200	WH 350 × 200	WH 250 × 150	WH 800 × 300
C4	WH 300 × 200	WH 300 × 300	WH 300 × 300	WH 350 × 300	B8	WH 350 × 200	WH 400 × 200	WH 600 × 300	WH 450 × 300
C5	WH 300 × 200	WH 300 × 300	WH 300 × 300	WH 300 × 300	B9	WH 350 × 200	WH 300 × 250	WH 350 × 175	WH 600 × 300
C6	WH 700 × 400	WH 600 × 300	WH 500 × 300	WH 500 × 400	B10	WH 700 × 300	WH 350 × 200	WH 350 × 175	WH 500 × 300
C7	WH 500 × 400	WH 450 × 300	WH 300 × 300	WH 400 × 300	P1	2.1	1.5	1.2	1.8
C8	WH 450 × 300	WH 300 × 300	WH 300 × 300	WH 350 × 300	P2	2.1	1.5	1	1.5
C9	WH 450 × 300	WH 300 × 300	WH 300 × 300	WH 350 × 300	P3	2	1.2	1	1.2
C10	WH 450 × 300	WH 300 × 300	WH 300 × 300	WH 300 × 300	P4	1.9	1	1	1.1
B1	WH 400 × 200	WH 250 × 200	WH 350 × 175	WH 300 × 200	P5	1.3	1	1	1
B2	WH 350 × 200	WH 350 × 200	WH 350 × 175	WH 400 × 200	FW*	121.74	113.49	102.28	139.41
B3	WH 400 × 200	WH 350 × 200	WH 250 × 150	WH 300 × 200	PF	14.21	19.56	19.53	22.71
B4	WH 350 × 200	WH 250 × 200	WH 350 × 175	WH 350 × 175	TW	135.95	133.05	121.81	162.12

FW*: steel frame weight; PW: steel plate weight; TW: total weight. The units of weight and thickness of SPSWs are kN and mm; respectively.

Table 6. Percentage of story shear resisted by steel plate in the optimum designs of 5-story steel frame (%).

Story	1	2	3	4	5	Average
SPSW1-5	67.95	69.22	62.13	52.05	38.68	58.01
SPSW2-5	72.59	67.81	63.76	52.79	38.96	59.18
SPSW3-5	55.86	72.9	69.62	57.9	39.96	59.25
SPSW3-5-SGA	52.02	70	64.01	46.42	40.17	54.52

The optimum weight of SPSW3-5 was 24.86% lower than that of SPSW3-5-SGA (162.12 kN). As shown in Figure 10, SGA converges prematurely and falls into a local optimal solution; while IGA can obtain a better solution than SGA by finding an efficient cross direction through DBHX, obtaining new individuals through a substitution operation, controlling the mutation scale by the adaptive mutation operator, and retaining the best individuals of each generation by the elite scheme.

Figure 10 shows the inter-story drift ratios of the five-story steel frame. The maximum and average stress ratios of the frame and plate elements with the five-story steel frame are presented in Table 7. It was observed that the maximum inter-story drift ratios and the maximum stress ratios of the frame and plate elements for SPSW1-5, SPSW2-5, SPSW3-5, and SPSW3-5-SGA did not exceed the allowable values of 0.004 and 1, respectively. In addition, the maximum and average stress ratios of the frame and plate elements of SPSW3-5 were larger than those of SPSW1-5 and SPSW2-5. Results show that the structural elements were more fully utilized in the layout optimization of SPSW3-5 than in the size optimization of SPSW1-5 and SPSW2-5 when their inter-story drift ratios meet the specification requirements. This demonstrates the superiority of SPSW3-5 over SPSW1-5 and SPSW2-5.

Figure 10. Inter-story drift ratio for optimum designs of 5-story steel frame.

Table 7. Maximum and average stress ratios of the frame and plate elements for structures with a 5-story steel frame.

Stress Ratios		SPSW1-5	SPSW2-5	SPSW3-5	SPSW3-5SGA
Frame	Max	0.9454	0.9146	0.9956	0.9319
elements	Average	0.7556	0.7457	0.7575	0.5641
Plate	Max	0.8489	0.7115	1	0.68
elements	Average	0.677	0.6446	0.8218	0.5802

The maximum and average stress ratios of the frame and plate elements of SPSW3-5 were larger than those of SPSW3-5-SGA, thereby indicating the superior performance of IGA compared with SGA.

3.3. Optimization Results of the 10-Story Steel Frame

Figures 11 and 12 show the best configuration of SPSW and convergence histories of the 10-story steel frame, respectively. Tables 8 and 9 present the details of the results and percentages of story shear resisted by the steel plates, respectively. As shown in Table 8, the total weights of the layout optimization of SPSW3-10 were 22.32% and 16.62% lighter than those of the size optimization of SPSW1-10 and SPSW2-10, respectively. Additionally, it can be found from these results in both Tables 8 and 9 show that the frame weight can be reduced by increasing the average percentage of story shear resisted by the steel plate.

As shown in Figure 13, the maximum inter-story drift ratios of SPSW1-10, SPSW2-10, and SPSW3-10 are 0.004, which is equal to the allowable value. In addition, Table 10 summarizes the maximum stress ratios of the frame and plate elements of SPSW1-10, SPSW2-10, and SPSW3-10 and are less than the allowable values of 1. The maximum and average stress ratios of the frame elements and steel plate elements of SPSW3-10 were larger than those of SPSW1-10 and SPSW2-10. Therefore, it can be concluded that the designs of SPSW1-10 and SPSW2-10 are dominated by inter-story drift ratios. Nevertheless, the design of SPSW3-10 was dominated by the inter-story drift ratios and element stress ratios. Under the limitation of inter-story drift ratios, the structural elements used in SPSW3-10 are more effective than those in SPSW1-10 and SPSW2-10. Therefore, SPSW3-10 has a superior design compared to those of SPSW1-10 and SPSW2-10.

P10		P10
P9	P9	P9
P8	P8	P8
P7		P7
P6		P6
P5		P5
P4	P4	P4
P3	P3	P3
P2		P2
P1		P1

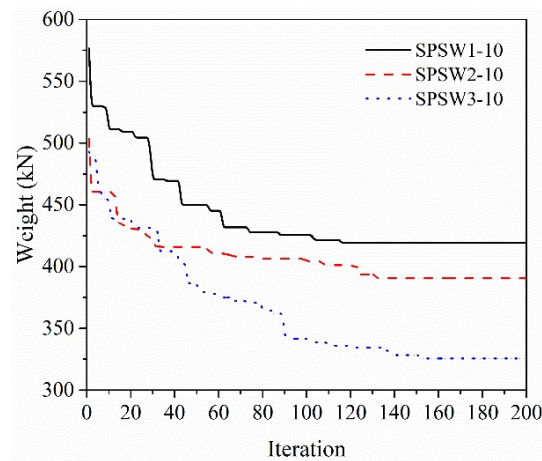**Figure 11.** Best configuration of SPSW of SPSW3-10.

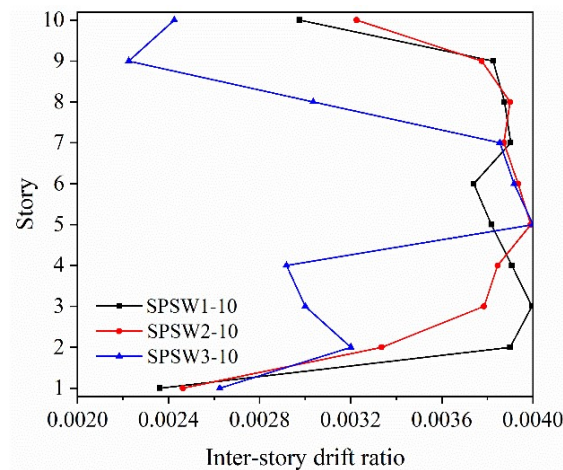**Figure 12.** Convergence histories of 10-story steel frame.

Figure 13. Inter-story drift ratio for optimum designs of 10-story steel frame.

Table 8. Optimum designs of 10-story steel frame.

No.	Optimum Designs			No.	Optimum Designs		
	SPSW1-10	**SPSW2-10**	**SPSW3-10**		**SPSW1-10**	**SPSW2-10**	**SPSW3-10**
C1	WH800 × 350	WH900 × 400	WH900 × 400	B8	WH600 × 300	WH400 × 300	WH250 × 200
C2	WH700 × 300	WH700 × 300	WH800 × 300	B9	WH600 × 300	WH400 × 300	WH250 × 200
C3	WH700 × 300	WH700 × 300	WH600 × 300	B10	WH600 × 300	WH800 × 300	WH700 × 300
C4	WH700 × 300	WH700 × 300	WH600 × 300	B11	WH350 × 300	WH300 × 200	WH300 × 200
C5	WH700 × 300	WH700 × 300	WH600 × 300	B12	WH350 × 300	WH400 × 200	WH800 × 300
C6	WH700 × 300	WH700 × 300	WH600 × 300	B13	WH400 × 250	WH500 × 250	WH250 × 200
C7	WH700 × 300	WH700 × 300	WH500 × 300	B14	WH350 × 250	WH500 × 300	WH800 × 300
C8	WH600 × 300	WH600 × 300	WH400 × 300	B15	WH350 × 200	WH600 × 300	WH400 × 250
C9	WH500 × 300	WH450 × 300	WH350 × 300	B16	WH400 × 300	WH600 × 300	WH400 × 200
C10	WH450 × 300	WH400 × 300	WH350 × 300	B17	WH300 × 300	WH600 × 300	WH800 × 300
C11	WH900 × 400	WH900 × 350	WH700 × 300	B18	WH300 × 300	WH600 × 300	WH250 × 200
C12	WH800 × 350	WH800 × 350	WH700 × 300	B19	WH400 × 200	WH500 × 300	WH700 × 300
C13	WH800 × 300	WH700 × 300	WH600 × 300	B20	WH700 × 300	WH500 × 300	WH300 × 200
C14	WH700 × 300	WH700 × 300	WH600 × 300	P1	3.2	2.1	1.6
C15	WH700 × 300	WH700 × 300	WH600 × 300	P2	3.2	2.1	1.6
C16	WH700 × 300	WH700 × 300	WH600 × 300	P3	3.2	2	1.5
C17	WH700 × 300	WH700 × 300	WH500 × 300	P4	3.2	2	1.5
C18	WH600 × 300	WH600 × 300	WH350 × 300	P5	3.2	2	1.5
C19	WH500 × 300	WH450 × 300	WH350 × 300	P6	3.1	2	1.5
C20	WH450 × 300	WH400 × 300	WH350 × 300	P7	2.9	1.8	1.5
B1	WH400 × 300	WH250 × 200	WH250 × 200	P8	2.6	1.5	1.5
B2	WH500 × 300	WH400 × 200	WH400 × 200	P9	2.3	1.5	1.3
B3	WH600 × 300	WH400 × 200	WH250 × 200	P10	1.2	1.5	1.2
B4	WH800 × 300	WH450 × 300	WH350 × 200	FW*	377.61	336.32	272.14
B5	WH800 × 300	WH450 × 250	WH400 × 200	PF	41.55	54.18	53.46
B6	WH700 × 300	WH400 × 300	WH400 × 200	TW	419.15	390.50	325.61
B7	WH600 × 300	WH400 × 300	WH400 × 200				

FW*: steel frame weight; PW: steel plates weight; TW: total weight. The units of weight and thickness of SPSWs are in kN and mm, respectively.

Table 9. Percentage of story shear resisted by steel plate in optimum designs of 10-story steel frame (%).

Story	1	2	3	4	5	6	7	8	9	10	Average
SPSW1-10	60.5	65.51	52.59	38.59	32.06	31.78	36.53	34.28	21.19	5.59	37.86
SPSW2-10	67.69	73.02	68.72	62.3	54.4	47.63	41.36	40.51	39.16	38.62	53.34
SPSW3-10	66.47	54.22	77.83	72.94	66.64	66.26	43.25	70.03	66.08	44.75	62.85

Table 10. Maximum and average stress ratios of frame and plate elements for 10-story steel frame.

Stress Ratios		**SPSW1-10**	**SPSW2-10**	**SPSW3-10**
Frame elements	Max	0.9475	0.9732	0.9969
	Average	0.6482	0.6446	0.6885
Plate elements	Max	0.7026	0.6911	0.9781
	Average	0.4438	0.4767	0.7417

3.4. Optimization Results of the 20-Story Steel Frame

Figures 14 and 15 show the best configuration of SPSW and convergence histories of the 20-story steel frame, respectively, where Table 11 summarizes the optimum results. The percentages of the story shear resisted by the steel plate are listed in Table 12.

The total best weights of SPSW3-20 were 26.06% and 17.89% lighter than those of SPSW1-20 and SPSW2-20, respectively. The average percentages of story shear resisted by SPSW3-20 (56.78%) were higher than that for SPSW1-20 (33.4%) and SPSW2-20 (44.35%). This indicates that the frame weight becomes significantly reduced when the average percentage of story shear resisted by the steel plates increases, which is similar to the case in which the frame layers are 5 or 10.
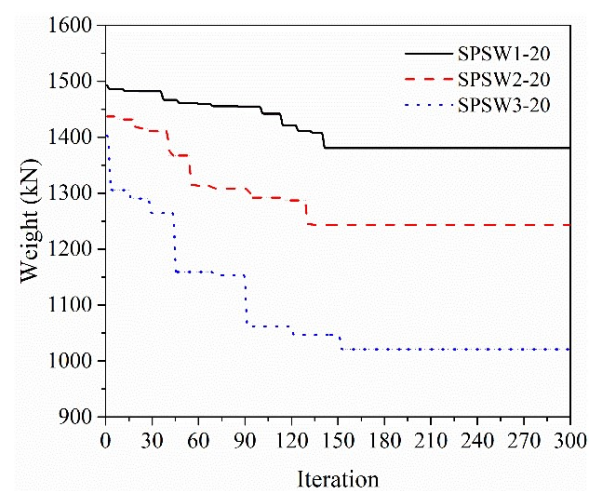
Figure 14. Best configuration of SPSW of SPSW3-20.

Figure 15. Convergence histories of 20-story steel frame.
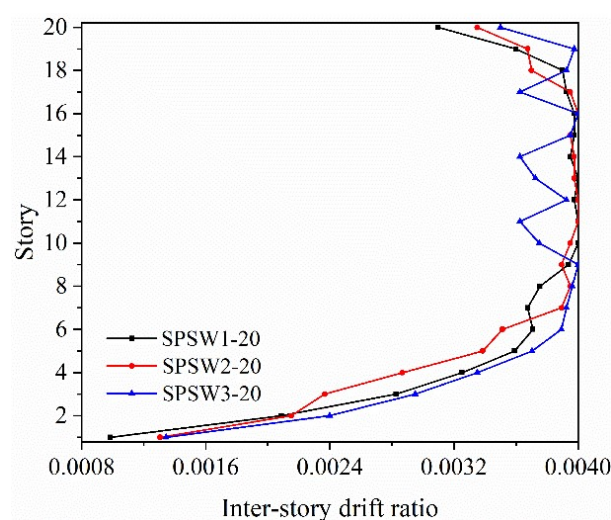
Table 11. Optimum designs of a 20-story steel frame.

No.	Optimum Designs			No.	Optimum Designs		
	SPSW1-20	SPSW2-20	SPSW3-20		SPSW1-20	SPSW2-20	SPSW3-20
C1	WH1500 × 550	WH1500 × 500	WH1500 × 550	B13	WH700 × 300	WH500 × 300	WH400 × 200
C2	WH1500 × 500	WH1400 × 500	WH1500 × 550	B14	WH800 × 300	WH500 × 300	WH400 × 200
C3	WH1500 × 500	WH1400 × 500	WH1400 × 500	B15	WH600 × 300	WH450 × 300	WH350 × 300
C4	WH1500 × 500	WH1200 × 500	WH1400 × 500	B16	WH800 × 300	WH400 × 300	WH300 × 250
C5	WH1300 × 500	WH1200 × 500	WH1200 × 450	B17	WH600 × 300	WH400 × 200	WH400 × 200
C6	WH1300 × 500	WH1200 × 500	WH1200 × 450	B18	WH800 × 300	WH400 × 200	WH350 × 200
C7	WH1300 × 500	WH1200 × 500	WH1200 × 400	B19	WH700 × 300	WH400 × 200	WH350 × 175
C8	WH1300 × 500	WH1200 × 500	WH1200 × 400	B20	WH700 × 300	WH800 × 300	WH600 × 300
C9	WH1300 × 500	WH1200 × 500	WH1200 × 400	B21	WH300 × 200	WH600 × 300	WH600 × 300
C10	WH1200 × 500	WH1200 × 500	WH1100 × 400	B22	WH300 × 200	WH700 × 300	WH600 × 300
C11	WH1200 × 450	WH1200 × 450	WH1100 × 400	B23	WH350 × 300	WH800 × 300	WH700 × 300
C12	WH1200 × 450	WH1200 × 450	WH1100 × 400	B24	WH350 × 300	WH800 × 300	WH600 × 300
C13	WH1200 × 450	WH1200 × 400	WH900 × 350	B25	WH350 × 175	WH600 × 300	WH700 × 300
C14	WH1100 × 400	WH1100 × 400	WH900 × 350	B26	WH400 × 250	WH800 × 300	WH600 × 300
C15	WH1100 × 400	WH1100 × 400	WH900 × 350	B27	WH450 × 300	WH700 × 300	WH600 × 300
C16	WH800 × 350	WH900 × 350	WH900 × 350	B28	WH450 × 300	WH700 × 300	WH700 × 300
C17	WH700 × 300	WH700 × 300	WH800 × 300	B29	WH400 × 300	WH800 × 300	WH800 × 300
C18	WH500 × 300	WH600 × 300	WH600 × 300	B30	WH450 × 250	WH800 × 300	WH400 × 200
C19	WH450 × 300	WH500 × 300	WH450 × 300	B31	WH300 × 250	WH800 × 300	WH800 × 300
C20	WH400 × 300	WH400 × 300	WH300 × 300	B32	WH350 × 300	WH800 × 300	WH800 × 300
C21	WH1500 × 550	WH1400 × 500	WH1400 × 500	B33	WH350 × 175	WH800 × 300	WH400 × 200
C22	WH1500 × 550	WH1400 × 500	WH1200 × 500	B34	WH400 × 300	WH700 × 300	WH800 × 300
C23	WH1500 × 500	WH1400 × 500	WH1100 × 400	B35	WH400 × 300	WH800 × 300	WH600 × 300
C24	WH1500 × 500	WH1200 × 450	WH800 × 350	B36	WH400 × 250	WH800 × 300	WH800 × 300
C25	WH1300 × 500	WH1200 × 450	WH800 × 350	B37	WH350 × 200	WH800 × 300	WH800 × 300
C26	WH1300 × 500	WH1200 × 450	WH800 × 350	B38	WH300 × 300	WH800 × 300	WH500 × 300
C27	WH1300 × 500	WH1200 × 400	WH800 × 350	B39	WH300 × 200	WH700 × 300	WH500 × 300
C28	WH1300 × 500	WH1200 × 400	WH800 × 350	B40	WH800 × 300	WH700 × 300	WH500 × 300
C29	WH1300 × 500	WH1200 × 400	WH800 × 350	P1	7	3.8	3
C30	WH1300 × 500	WH1200 × 400	WH800 × 350	P2	6.8	3.8	3
C31	WH1200 × 500	WH1200 × 400	WH800 × 350	P3	6.4	3.8	3
C32	WH1200 × 500	WH1200 × 400	WH800 × 350	P4	6.3	3.6	2.9
C33	WH1200 × 500	WH1200 × 400	WH700 × 300	P5	6	3.6	2.9
C34	WH1200 × 450	WH1200 × 400	WH700 × 300	P6	5.4	3.4	2.9
C35	WH1200 × 450	WH1100 × 400	WH600 × 300	P7	4.9	3.4	2.9
C36	WH900 × 350	WH900 × 350	WH600 × 300	P8	4.7	3.2	2.9
C37	WH700 × 300	WH800 × 350	WH600 × 300	P9	4.5	3	2.3
C38	WH600 × 300	WH800 × 300	WH600 × 300	P10	3.9	3	2
C39	WH500 × 300	WH500 × 300	WH450 × 300	P11	3.6	3	2
C40	WH450 × 300	WH400 × 300	WH300 × 300	P12	3.3	2.8	2
B1	WH600 × 300	WH400 × 200	WH350 × 200	P13	3.2	2.8	2
B2	WH700 × 300	WH400 × 200	WH350 × 200	P14	2.8	2.8	2
B3	WH500 × 300	WH450 × 300	WH350 × 175	P15	2.6	2.5	2
B4	WH700 × 300	WH450 × 300	WH350 × 200	P16	2.4	2.2	2
B5	WH600 × 300	WH400 × 200	WH300 × 200	P17	2.4	2	1.7
B6	WH700 × 300	WH450 × 300	WH350 × 175	P18	2.1	1.8	1.2
B7	WH800 × 300	WH400 × 200	WH350 × 200	P19	1.8	1.6	1
B8	WH800 × 300	WH400 × 200	WH350 × 300	P20	1.5	1.5	1
B9	WH600 × 300	WH450 × 300	WH350 × 250	FW*	1273.06	1090.64	881.96
B10	WH800 × 300	WH500 × 300	WH400 × 200	PW	107.61	152.61	138.92
B11	WH800 × 300	WH500 × 300	WH400 × 200	TW	1380.67	1243.25	1020.88
B12	WH800 × 300	WH500 × 300	WH400 × 200				

FW*: steel frame weight; PW: steel plates weight; TW: total weight. The units of weight and thickness of SPSWs are kN and mm, respectively.

As shown in Figure 16 and Table 13, the maximum inter-story drift ratios of SPSW1-20, SPSW2-20, and SPSW3-20 is 0.004, which is equal to the allowable value. The maximum and average stress ratios of the frame and plate elements for SPSW3-20 were larger than those for SPSW2-20 and SPSW3-20. This indicates that the inter-story drift ratio dominates the design in the size optimization of SPSW1-20 and SPSW2-20. However, in the layout optimization of SPSW3-20, both the inter-story drift ratios and element stress ratios dominate the design. The structural elements of SPSW3-20 are more fully utilized than those of SPSW1-20 and SPSW2-20 under the limitation of inter-story drift ratios. Thus, the superiority of SPSW3-20 over SPSW1-20 and SPSW2-20 was established.

Table 12. Percentage of story shear resisted by steel plate in optimum designs of 20-story steel frame (%).

Story	SPSW1-20	SPSW2-20	SPSW3-20	Story	SPSW1-20	SPSW2-20	SPSW3-20
1	44.56	45.51	42.13	11	28.69	43.92	70.42
2	63.57	61.81	60.3	12	26.04	41.41	40.67
3	53.36	58.36	63.25	13	26.5	40.19	73.19
4	52.67	59.07	64.97	14	24.77	39.69	67.39
5	51.05	62.61	63.18	15	27.73	35.72	55.69
6	44.01	55.02	63.21	16	23.4	32.16	37.67
7	37.29	55.46	63.67	17	27.06	25.23	64.54
8	36.73	52.39	60	18	19.18	20.12	40.77
9	38.54	47.59	42.02	19	6.57	25.92	42.1
10	34.42	46.33	76.77	20	3.8	38.54	43.69
				Average	33.4	44.35	56.78

Figure 16. Inter-story drift ratio for optimum designs of 20-story steel frame.

Table 13. Maximum and average stress ratios of frame and plate elements for the 20-story steel frame.

Stress Ratios		SPSW1-20	SPSW2-20	SPSW3-20
Frame elements	Max	0.9349	0.8366	0.9939
	Average	0.5044	0.4987	0.5769
Plate elements	Max	0.6275	0.3952	0.7678
	Average	0.3128	0.3042	0.4849

4. Conclusions

This study entailed the development of an IGA to optimize the placement of SPSWs in steel frames. To accurately model the performance of the SPSWs, SM and CSM were used for evaluation considering different height-to-thickness ratios λ. Furthermore, three optimization examples of 5-, 10-, and 20-story steel frames were analyzed to investigate the performance of steel frames with conventional and optimal configurations of SPSW. For each layer, two cases of size optimization of frames with conventional configurations of SPSW (SPSW1 and SPSW2) and one case of layout optimization were conducted to determine the optimal placement of SPSWs in the frame (SPSW3). To verify the superiority of IGA over SGA, the layout optimization of the five-story steel frame was conducted to determine the optimal configuration of an SPSW using SGA. The following conclusions were drawn from the analysis of this study:

- In the five-story steel frames, the total weight of the layout optimization of SPSW3-5 was 10.4% and 8.45% lighter than those of the size optimization of SPSW1-5 and

　　　SPSW2-5, respectively. In the 10-story steel frames, the total optimal weights of SPSW3-10 were 22.32% and 16.62% lighter than those of SPSW1-10 and SPSW2-10, respectively. In the 20-story steel frames, the total best weights of SPSW3-20 were 26.06% and 17.89% lighter than those of SPSW1-20 and SPSW2-20, respectively. As the number of layers increased, the total weight reduction of the structures became more evident.

- The total weight of the layout optimization of SPSW3-5 using IGA was 24.86% lighter than that of SPSW3-5-SGA using SGA. In addition, the maximum and average stress ratios of the frame and plate elements of SPSW3-5 were larger than those of SPSW3-5-SGA, indicating that the IGA is better than SGA.

- In each example, the average percentages of story shear resisted by the web plates for SPSW3 were larger than those of SPSW1 and SPSW2. As the average percentage of story shear resisted by the web plates increased, a remarkable reduction in the steel frame weight was observed.

- In each example, the maximum and average stress ratios of the frame and plate elements of SPSW3 were larger than those of SPSW1 and SPSW2. Particularly, the average stress ratios of the plate elements of SPSW3 were approximately 0.15-0.3 higher than those of SPSW1 and SPSW2. This indicated that, in the layout optimization of SPSW3, the structural elements, especially the plate elements, were more fully utilized than in the size optimization of SPSW1 and SPSW2 when their inter-story drift ratios met the specification requirements.

- In each example in the two cases of SPSW1 and SPSW2, inter-story drift dominated the design. However, for SPSW3, the design was dominated by both the inter-story drift and member stress ratios. This highlighted the superiority of SPSW3 over SPSW1 and SPSW2.

　　　In summary, compared with one with the layout optimization using SGA and the others by size optimization, the SPSW system obtained by the IGA had obvious advantages in terms of material, horizontal load resistance, and ductility. However, the optimization in this study only considered static loads that acted on the structure system and did not completely consider the controlling indicators for high-rise buildings. Further optimization research should introduce dynamic loads into optimization models to examine the layout optimization for SPSW systems under dynamic action and comprehensively consider the controlling indicators for high-rise buildings.

Author Contributions: Conceptualization, J.H. and S.L.; methodology, S.L.; formal analysis, S.L.; data curation, S.L.; writing—original draft preparation, S.L.; writing—review and editing, Y.L. and S.C.; visualization, X.D. and S.C.; supervision, J.H.; project administration, J.H. and S.C.; funding acquisition, J.H. All authors have read and agreed to the published version of the manuscript.

Institutional Review Board Statement: Not applicable.

Informed Consent Statement: Not applicable.

Data Availability Statement: Not applicable.

Conflicts of Interest: The authors declare no conflict of interest.

References

1. Toğan, V. Design of planar steel frames using Teaching-Learning Based Optimization. *Eng. Struct.* **2012**, *34*, 225–232. [CrossRef]
2. Çarbaş, S. Optimum structural design of spatial steel frames via biogeography-based optimization. *Neural. Comput. Appl.* **2017**, *28*, 1525–1539. [CrossRef]
3. Kaveh, A.; Farhoodi, N. Layout optimization for X-bracing of planar steel frames using ant system. *Int. J. Civ. Eng.* **2010**, *8*, 256–275.
4. Kaveh, A.; Farhoudi, N. A unified approach to parameter selection in meta-heuristic algorithms for layout optimization. *J. Constr. Steel Res.* **2011**, *67*, 1453–1462. [CrossRef]
5. Liang, Q.; Xie, Y.; Steven, G. Optimal topology design of bracing systems for multistory steel frames. *J. Struct. Eng.* **2000**, *126*, 823–829. [CrossRef]

6. Bagherinejad, M.H.; Haghollahi, A. Topology optimization of steel plate shear walls in the moment frames. *Steel Compos. Struct. Int. J.* **2018**, *29*, 767–779. [CrossRef]

7. Gholizadeh, S.; Fattahi, F. Design optimization of tall steel buildings by a modified particle swarm algorithm. *Struct. Des. Tall Spec Build.* **2014**, *23*, 285–301. [CrossRef]

8. Farzampour, A.; Khatibinia, M.; Mansouri, I. Shape optimization of butterfly-shaped shear links using Grey Wolf algorithm. *Ing. Sismica* **2019**, *36*, 27–41. Available online: http://hdl.handle.net/10919/89385 (accessed on 13 May 2022).

9. Kim, Y.; Mortazavi, S.J.; Farzampour, A.; Hu, J.; Mansouri, I.; Awoyera, P.O. Optimization of the Curved Metal Damper to Improve Structural Energy Dissipation Capacity. *Buildings* **2022**, *12*, 67. [CrossRef]

10. Farzampour, A.; Eatherton, M.; Mansouri, I.; Hu, J. Effect of flexural and shear stresses simultaneously for optimized design of butterfly-shaped dampers: Computational study. *Smart Struct. Syst.* **2019**, *23*, 329–335.

11. Sabelli, R.; Bruneau, M. *Steel Plate Shear Walls (AISC Design Guide 20)*; American Institute of Steel Construction: Chicago, IL, USA, 2007.

12. Wang, M.; Shi, Y.J.; Xu, J.; Yang, W.G.; Li, Y.X. Experimental and numerical study of unstiffened steel plate shear wall structures. *J. Constr. Steel Res.* **2015**, *112*, 373–386. [CrossRef]

13. Alavi, E.; Nateghi, F. Experimental study on diagonally stiffened steel plate shear walls with central perforation. *J. Constr. Steel Res.* **2013**, *89*, 9–20. [CrossRef]

14. Ali, M.M.; Osman, S.A.; Husam, O.A.; Ai-Zand, A.W. Numerical study of the cyclic behavior of steel plate shear wall systems (SPSWs) with differently shaped opening. *Steel Compos. Struct. Int. J.* **2018**, *26*, 361–373.

15. Mansouri, I.; Arabzadeh, A.; Farzampour, A.; Hu, J. Seismic behavior investigation of the steel multi-story moment frames with steel plate shear walls. *Steel Compos. Struct.* **2020**, *37*, 91–98.

16. Curkovic, I.; Skejic, D.; Dzeba, I. Seismic performance of steel plate shear walls with variable column flexural stiffness. *Steel Compos. Struct. Int. J.* **2019**, *33*, 1–18. [CrossRef]

17. Curkovic, I.; Skejic, D.; Dzeba, I.; Matteis, G.D. Seismic performance of composite plate shear walls with variable column flexural stiffness. *Steel Compos. Struct. Int. J.* **2019**, *33*, 19–36. [CrossRef]

18. Shekastehband, B.; Azaraxsh, A.A.; Showkati, H. Hysteretic behavior of perforated steel plate shear walls with beam-only connected infill plates. *Steel Compos. Struct. Int. J.* **2017**, *25*, 505–521. [CrossRef]

19. Paslar, N.; Farzampour, A.; Hatami, F. Infill plate interconnection effects on the structural behavior of steel plate shear walls. *Thin-Walled Struct.* **2020**, *149*, 106621. [CrossRef]

20. Paslar, N.; Farzampour, A.; Hatami, F. Investigation of the infill plate boundary condition effects on the overall performance of the steel plate shear walls with circular openings. *Structures* **2020**, *27*, 824–836. [CrossRef]

21. Thorburn, L.J.; Kulak, G.L.; Montgomery, C.J. Analysis of steel plate shear walls. In *No. 107 of Structural Engineering Report*; University of Alberta: Edmonton, AB, Canada, 1983.

22. Shishkin, J.J.; Driver, R.G.; Grondin, G.Y. Analysis of steel plate shear walls using the modified strip model. *J. Struct. Eng.* **2009**, *135*, 1357–1366. [CrossRef]

23. Guo, L.H.; Li, R.; Zhang, S.M.; Yan, G.R. Hysteretic analysis of steel plate shear walls (SPSWs) and a modified strip model for SPSWs. *Adv. Struct. Eng.* **2012**, *15*, 1751–1764. [CrossRef]

24. Chatterjee, A.K.; Bhowmick, A.; Bagchi, A. Development of a simplified equivalent braced frame model for steel plate shear wall systems. *Steel Compos. Struct.* **2015**, *18*, 711–737. [CrossRef]

25. Gholizadeh, S.; Shahrezaei, A.M. Optimal placement of steel plate shear walls for steel frames by bat algorithm. *Struct. Des. Tall Spec. Build.* **2015**, *24*, 1–18. [CrossRef]

26. *AISC 341-2010*; Seismic Provisions for Structural Steel Buildings. American Institute of Steel Construction: Chicago, IL, USA, 2010.

27. *JGJ/T 380-2015*; Technical Specification for Steel Plate Shear Walls. China Architecture and Building Press: Beijing, China, 2015.

28. Elgaaly, M.; Caccese, V.; Du, C. Postbuckling behavior of steel-plate shear walls under cyclic loads. *J. Struct. Eng.* **1993**, *119*, 588–605. [CrossRef]

29. *CAN/CSA S16.1-01*; Limit States Design of Steel Structures. Canadian Standards Association: Toronto, ON, Canada, 2001.

30. Guo, L.H.; Jia, M.M.; Li, R.; Zhang, S.M. Hysteretic analysis of thin steel plate shear walls. *Int. J. Steel. Struct.* **2013**, *13*, 163–174. [CrossRef]

31. *GB 50017-2018*; Standard for Design of Steel Structures. China Planning Press: Beijing, China, 2018.

32. *GB 50011-2010*; Code for Seismic Design of Building. China Architecture and Building Press: Beijing, China, 2010.

33. Wang, J.Q.; Cheng, Z.W.; Zhang, P.L.; Dai, W.T. Research on improvement of real-coded genetic algorithm for solving constrained optimization problems. *Control Decis.* **2019**, *34*, 937–946.

34. Chuang, Y.C.; Chen, C.T.; Hwang, C. A simple and efficient real-coded genetic algorithm for constrained optimization. *Appl Soft Comput.* **2016**, *38*, 87–105. [CrossRef]

35. Zhang, Y. Optimization Design of Space Steel Frame Supporting System Based on Dynamic Performance. Master's Thesis, Guangdong University of Technology, Guangzhou, China, 2018.

36. De Jong, K.A. An Analysis of the Behavior of a Class of Genetic Adaptive Systems. Doctoral Dissertation, University of Michigan, University Microfilms, Ann Arbor, MI, USA, 1975.
37. MATLAB. *MATLAB 2010b*; Mathworks: Natick, MA, USA, 2010.
38. ANSYS. *ANSYS Version 14.0 Documentation*; ANSYS Inc.: Canonsburg, PA, USA, 2011.
39. *YB 3301-2005*; The Welded Steel H-Section. China Architecture and Building Press: Beijing, China, 2005.